Role of plasma-induced defects in the generation of 1/f noise in graphene

Applied Physics Letters

Role of plasma-induced defects in the generation of 1/*f* noise in graphene

Cite as: Appl. Phys. Lett. **112**, 093504 (2018); https://doi.org/10.1063/1.5024218
Submitted: 30 January 2018 . Accepted: 19 February 2018 . Published Online: 02 March 2018

Alessandro Cultrera, Luca Callegaro, Martina Marzano, Massimo Ortolano, and Giampiero Amato

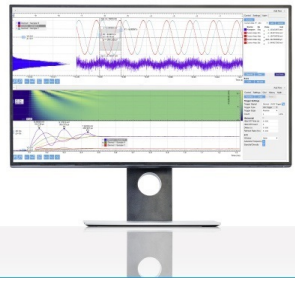

AIP Publishing

Role of plasma-induced defects in the generation of 1/*f* noise in graphene

Alessandro Cultrera,[1,a)] Luca Callegaro,[1] Martina Marzano,[1,2] Massimo Ortolano,[2,1] and Giampiero Amato[1,3]
[1]*INRIM - Istituto Nazionale di Ricerca Metrologica Strada delle Cacce 91, 10135 Torino, Italy*
[2]*Dipartimento di Elettronica e Telecomunicazioni, Politecnico di Torino, Corso Duca degli Abruzzi 24, 10129 Torino, Italy*
[3]*Dipartimento di Scienze e Innovazione Tecnologica, Università del Piemonte Orientale "A. Avogadro", viale T. Michel 11, 15121 Alessandria, Italy*

(Received 30 January 2018; accepted 19 February 2018; published online 2 March 2018)

It has already been reported that 1/*f* noise in graphene can be dominated by fluctuations of charge carrier mobility. We show here that the increasing damage induced by oxygen plasma on graphene samples result in two trends: at low doses, the magnitude of the 1/*f* noise increases with the dose; and at high doses, it decreases with the dose. This behaviour is interpreted in the framework of 1/*f* noise generated by carrier mobility fluctuations where the concentration of mobility fluctuation centers and the mean free path of the carriers are competing factors. *Published by AIP Publishing.*
https://doi.org/10.1063/1.5024218

Since the advent of graphene-based devices, several groups studied the effects of plasma treatments, mainly oxygen or argon, in order to lower the contact resistance between graphene and metallic electrodes, by means of controlled damage.[1–6] Plasma exposure from a few seconds to few tens of seconds are generally reported to substantially improve the electric contact quality.

We present a study on the behaviour of 1/*f* noise in graphene damaged by increasing exposure to oxygen plasma dose. We found that there are two trends: at low doses, the magnitude of the 1/*f* noise increases with the dose, whereas at high doses, the magnitude of the 1/*f* noise is a decreasing function of the dose. This result is interpreted in the framework of 1/*f* noise generated by carrier mobility fluctuations where the concentration of mobility fluctuation centers and the mean free path of the carriers are competing factors.

Electrical excess noise is a parameter of interest for the characterization of electronic devices, including recently developed graphene-based sensors.[7–10] In particular, 1/*f* noise constitutes a fundamental limit to the resolution of resistive[11] and Hall effect sensors,[12,13] and the frequency up-conversion of 1/*f* noise affects amplitude and phase noise of radio-frequency amplifiers, oscillators, and detectors.[11] Graphene sensors having electrical noise as output were also proposed.[14–17] As for other materials, the origin of 1/*f* noise in graphene is not completely understood and subject of considerable debate (see Ref. 11 for a review).

The correlation of 1/*f* noise magnitude with the amount and type of defect in graphene remains obscure. Hossain *et al.*[18] report that the magnitude of 1/*f* noise decreases with increasing damage caused by electron irradiation. In this work, we repeatedly exposed graphene samples to oxygen plasma. The measured 1/*f* noise magnitude shows a non-monotonic behaviour versus the increasing plasma dose, which can be correlated with the type and amount of damage quantified by Raman spectroscopy.

For the preparation of the samples, we used commercial graphene grown by chemical vapor deposition on Cu and then transferred on SiO_2/Si wafer. The plasma etching process was performed in a low pressure atmosphere of oxygen (during the exposition, the pressure was about 10^{-3} mbar) at 10 W RF power and 2.5 SCCM[19] oxygen flow for an exposure time of $t_P = 5$ s at each repetition.[20] With these parameters, it is possible to damage the graphene in a controlled way, avoiding the amorphization of the material due to the substitution of sp^2 bonds with sp^3 ones.[21]

The power spectral density (PSD) $S_v(f)$ of the voltage fluctuations was measured with a digital correlation spectrum analyzer, already employed in Johnson noise thermometry experiments.[22] The sample was excited with a low-noise DC current I.[23] The noise voltage across the sample was simultaneously amplified by two AC-coupled, two-stage low-noise amplifiers[24] and digitized by a two-channel analogue-to-digital converter board operating at a sampling frequency of 20 kHz.[25] All samples were recorded for off-line processing. Cross periodograms, which reject amplifiers' noise to a large extent,[26] were computed using Bartlett's method.[27] The typical measurement involves vectors of 2^{17} voltage sample pairs, providing estimates of the voltage noise cross PSD $S_v(f)$ for $f \approx k \times 0.153$ Hz, where $k = 1, \ldots, 2^{16}$. All measurements were performed in a shielded environment at $T = 296.0(5)$ K.

Figure 1 reports, as an example, the voltage noise PSDs corresponding to three different stages of the experiment. These PSDs show a combination of two noise components: a white noise component at high frequency and a 1/*f* component at low frequency, with PSD

$$S_v(f) \approx \mathbb{S}_v / f^{\alpha}, \tag{1}$$

α being a constant close to 1 and $\mathbb{S}_v$ characterizing the voltage noise magnitude. From Fig. 1, it can be observed that the crossover between the two components is at about 100 Hz. The white component of the PSD allows us to estimate the sample resistance as $R = \langle v^2 \rangle / (4 k_B T B)$, where $\langle v^2 \rangle$ is the noise power over the bandwidth B and k_B is the Boltzmann constant. Here, we take $B = 3$ kHz–7 kHz. For the 1/*f* component, assuming that it is due to resistance fluctuations,[28,29] the relation

a)Electronic mail: a.cultrera@inrim.it

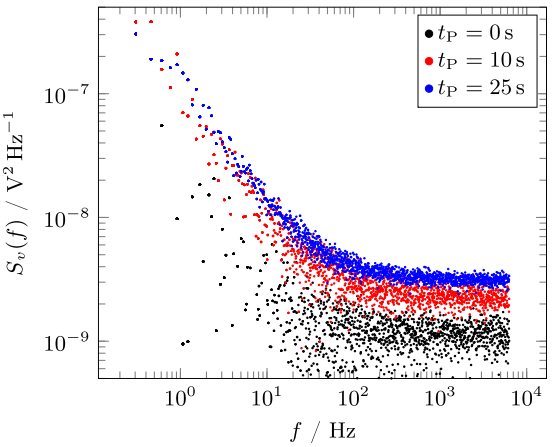

FIG. 1. Voltage noise spectra corresponding to an oxygen plasma exposure time t_P of 0 s (pristine), 10 s, and 25 s.

$$\frac{S_v(f)}{V^2} = \frac{S_r(f)}{R^2} \tag{2}$$

holds between the PSD $S_v(f)$, normalized to the square of the DC voltage V across the sample, and the PSD $S_r(f)$ of the resistance fluctuations, normalized to the sample resistance R squared. Given the relations in Eqs. (1) and (2), we can define the normalized noise magnitude at 1 Hz as

$$\mathbb{S} = \frac{\mathbb{S}_v}{V^2} = \frac{\mathbb{S}_r}{R^2}, \tag{3}$$

where $\mathbb{S}_r$ is the resistance noise magnitude and $\mathbb{S}$ is representative of the material condition at each stage of the experiment; $\mathbb{S}$ will be used as a first parameter of interest in the following discussion. The level of damage caused by the exposure to oxygen plasma was estimated by means of Macro-Raman spectroscopy, which allows the phenomenological determination of the average distance between the defects. Raman spectra were collected by a tool[30] equipped with a laser source of wavelength $\lambda_L = 532\,nm$, focused onto a spot with a diameter of 100 μm. The relatively wide laser spot allowed us to investigate relatively large areas of the sample, averaging over possible pristine structural inhomogeneities of the sample. For the acquisition of each Raman spectrum, the sample was exposed for 60 s to a power density of 150 W cm^{-2}.[31] This is important to avoid the formation of unwanted additional laser-induced defects during the characterisation.[32] The three Raman spectra shown in Fig. 2 correspond to the three voltage noise spectra shown in Fig. 1. The peaks D (defective), G (graphitic), and 2D (D overtone) are located at about 1350 cm^{-1}, 1590 cm^{-1}, and 2700 cm^{-1}, respectively.[33,34] Figure 2 shows that exposure to oxygen plasma provokes structural changes in graphene; these can be assessed through the evolution of the above mentioned Raman signatures, in particular, the monotonic increase of the D mode and the broadening of the 2D mode. The growth of the D mode indicates the appearance of vacancy- or point-like defects,[35] while the 2D mode broadening gives information about the weak nano-metre scale distortion of the carbon honeycomb lattice.[36] The two phenomena are competitive. The structural changes in the graphene samples due to the appearance of point-like defects

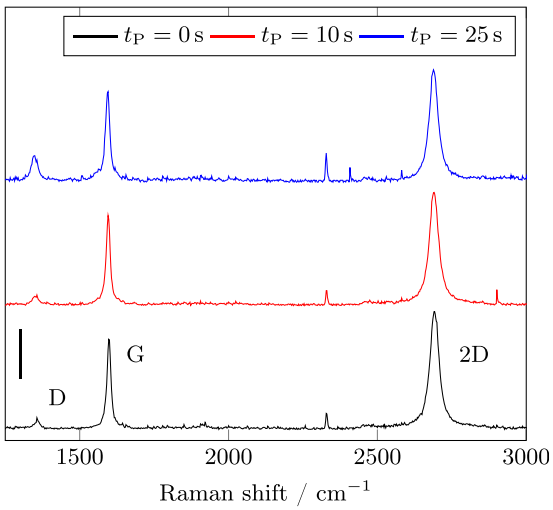

FIG. 2. Evolution of Raman signatures in graphene sample before ($t_P = 0\,s$, pristine) and after 10 s and 25 s of exposure to oxygen plasma. The feature at about 2300 cm^{-1} is due to the atmospheric nitrogen along the optical path of the laser beam. The vertical marker at the bottom left represents 2×10^3 counts.

can be assessed by the average point-defect distance L_D, which can be calculated from the Raman spectra following the Tuinstra-Koenig[37,38] relation

$$L_D^2 = (1.8 \times 10^{-9} nm^{-2}) \lambda_L^4 \frac{I_G}{I_D}, \tag{4}$$

where the numerical factor in the right hand side of Eq. (4) is empirical, λ_L is the laser wavelength (in nm), and I_G/I_D is the intensity ratio between the G and D peaks of the Raman spectrum. This law is considered accurate down to a defect distance of about 10 nm.[39] On the other side, the more "gentle" structural change due to weak lattice distortion can be observed following the evolution of the 2D peak full width at half maximum (FWHM). In Fig. 3, a broadening of the 2 D feature within the first damaging cycles can be observed.[40]

Note that L_D is calculated from the I_G/I_D ratio and the D peak is only sensitive to defects being directly related to the presence of unsaturated bonds.[41] This means that in the case of weak lattice distortion, the D peak is less informative about changes in the material. Conversely, the 2D peak broadens prior to the appearance of a strong D signature.[36]

As a third parameter of interest, we consider the mean free path l_0 of a free carrier in our samples. It was calculated from the measured field effect mobility of the graphene. In our samples, the mobility is of the order of 10^3 $cm^2\,V^{-1}\,s^{-1}$ for the pristine material and was obtained from back gate field effect measurements, while the carrier concentration n of the order of $3 \times 10^{13}\,cm^{-1}$ was calculated from mobility and resistance measurements. To calculate the mean free carrier path, consider the following. The semiclassical approximation for the electrical conductivity σ_{sc} is (see Ref. 42)

$$\sigma_{sc} = e^2 \tau \frac{n}{m^*}, \tag{5}$$

where e is the elementary charge, τ is the carrier scattering time, and n is the carrier concentration. The definition of

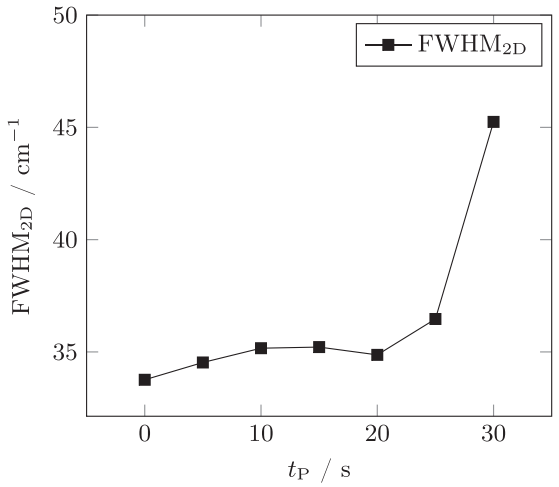

FIG. 3. Full width at half maximum of the 2D peak as a function of the oxygen plasma exposure time t_P.

effective mass m^* to be used in the semiclassical approximation for graphene is (Ref. 43, Sec. II)

$$m^* = \frac{\hbar k_F}{v_F} = \frac{\hbar\sqrt{\pi n}}{v_F}, \tag{6}$$

where $\hbar k_F$ and v_F are the Fermi momentum and velocity, respectively, and μ is the carrier mobility. Now, since the conductivity can also be written as

$$\sigma_{sc} = \mu e n \tag{7}$$

and

$$l_0 = v_F \tau, \tag{8}$$

the following relation yields the mean free path:

$$l_0 = \frac{\hbar}{e}\mu\sqrt{n\pi}. \tag{9}$$

Figure 4 reports the three parameters of interest—the resistance noise magnitude at 1 Hz $\mathbb{S}$, the average point-defect distance L_D, and the carrier mean free path l_0—as a function of exposure time t_P to the oxygen plasma. The mean free path and defect distance have a monotonic behavior, while $\mathbb{S}$ initially increases up to a maximum for $t_P = 10$ s and then decreases for longer plasma exposure time.

We distinguish between two regimes: in regime $\mathcal{A}$ at low exposure time, $t_P < 10$ s, l_0 decreases while L_D is approximatively constant and $\mathbb{S}$ increases; in regime $\mathcal{B}$ at high exposure time, $t_P > 10$ s, the defect distance L_D becomes comparable to the mean free path l_0 and $\mathbb{S}$ decreases. The fact that initially l_0 decreases even though L_D remains quite constant is not surprising. The carrier mean free path decreases as more defects pile up in the material irrespective of their type. It is then advisable to assume that in regime $\mathcal{A}$, the (decreasing) carrier mean free path is mainly affected by the (increasing) weak nanometre-scale distortion of the lattice rather than by the appearance of point-like defects as occurs in regime $\mathcal{B}$.

In a commonly accepted picture for graphene,[11,44] the 1/*f* noise is due to the fluctuation of the number of charges trapped in the substrate which act as long-range Coulomb

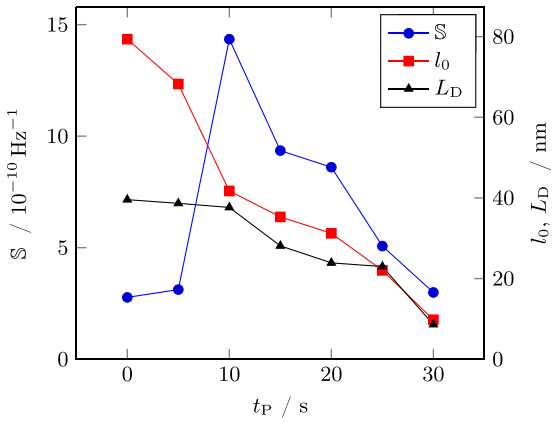

FIG. 4. Resistance noise magnitude at 1 Hz $\mathbb{S}$ (blue filled circle), carrier mean free path l_0 (red filled square), and average defect distance L_D (black filled triangle), as a function of the oxygen plasma exposure time t_P.

scatterers and induce resistance fluctuations in the graphene channel. This seems to be the dominant mechanism in exfoliated graphene at a low carrier concentration. Conversely, the CVD growth process yields a material with considerably larger disorder and doping than the exfoliated type. Hence, in CVD graphene, the short-range scattering becomes more important. Since at a large carrier concentration the long-range Coulomb potentials are screened, the role of the substrate is less important and the mobility fluctuations are largely due to scattering within the graphene itself.[45]

The following equation adapted from Ref. 46 (originally proposed in Ref. 47) provides a model for systems in which resistance noise is dominated by mobility fluctuations and where the 1/*f* noise emerges as a superposition of multiple processes with a wide distribution of characteristic time constants

$$\frac{S_r(f)}{R^2} = \frac{\mathbb{S}}{f} = \sum_\tau \frac{N_\mu}{\mathcal{V}} \frac{\tau\zeta(1-\zeta)}{1+(2\pi f\tau)^2} l_0^2(\sigma_1-\sigma_2)^2. \tag{10}$$

In this equation, $\mathcal{V}$ is the sample volume, τ is the characteristic time constant of the elementary process, N_μ is the concentration of centers that contribute to mobility fluctuations, and ζ is the probability for a N_μ center to be in a state with cross-section σ_1 (while $1-\zeta$ is the probability to be in a state with cross-section σ_2). Following this model, the resistance noise is proportional to the concentration N_μ and the mean free path l_0. In general, N_μ represents metastable lattice centers,[48] like the ones that occur in the first stage of damaging in our samples.

Our findings are in agreement with this model. The quantity l_0 decreases monotonically since it is sensitive to all types of defects. In regime $\mathcal{A}$, the constancy of L_D and the broadening of the 2D peak suggest that the main type of induced defect is that associated with mobility fluctuations, leading to an increase in N_μ. The behavior of $\mathbb{S}$ in regime $\mathcal{A}$ can be explained in terms of a positive contribution of N_μ, which countervails the effect of a decreasing l_0. Conversely, in regime $\mathcal{B}$, the average point-defect distance L_D decreases due to the appearance of a different type of defect which does not contribute to $\mathbb{S}$ anymore, which consequently starts to decrease following l_0. The present work indicates that 1/*f*

noise can be ascribed to mobility fluctuations in CVD graphene samples exposed to oxygen plasma treatments. This confirms and extends earlier observations[18] on exfoliated graphene samples damaged by an electron beam. Since a lot of fabrication processes involve plasma treatments, the present results indicate that this practice may increase the $1/f$ noise in graphene-based devices for short exposure time.

[1]S. K. Hong, J. G. Oh, W. S. Hwang, and B. J. Cho, Semicond. Sci. Technol. **32**, 045009 (2017).
[2]Q. Lu, Y. Liu, G. Han, C. Fang, Y. Shao, J. Zhang, and Y. Hao, Superlattices Microstruct. **1**, 421–427 (2017).
[3]J. A. Robinson, M. LaBella, M. Zhu, M. Hollander, R. Kasarda, Z. Hughes, K. Trumbull, R. Cavalero, and D. Snyder, Appl. Phys. Lett. **98**, 053103 (2011).
[4]D. Yue, C. Ra, X. Liu, D. Lee, and W. Yoo, Nanoscale **7**, 825 (2015).
[5]C.-H. Ra, M. S. Choi, D. Lee, and W. J. Yoo, J. Korean Inst. Surf. Eng. **49**, 152 (2016).
[6]M. S. Choi, S. H. Lee, and W. J. Yoo, J. Appl. Phys. **110**, 073305 (2011).
[7]S. Grover, S. Dubey, J. P. Mathew, and M. M. Deshmukh, Appl. Phys. Lett. **106**, 051113 (2015).
[8]T. Wang, D. Huang, Z. Yang, S. Xu, G. He, X. Li, N. Hu, G. Yin, D. He, and L. Zhang, Nano-Micro Lett. **8**, 95 (2016).
[9]S. El-Ahmar, W. Koczorowski, A. A. Poźniak, P. Kuświk, W. Strupiński, and R. Czajka, Appl. Phys. Lett. **110**, 043503 (2017).
[10]A. Nakamura, T. Hamanishi, S. Kawakami, and M. Takeda, Mater. Sci. Eng. B **219**, 20 (2017).
[11]A. A. Balandin, Nat. Nanotechnol. **8**, 549 (2013).
[12]H. Xu, L. Huang, Z. Zhang, B. Chen, H. Zhong, and L.-M. Peng, Appl. Phys. Lett. **103**, 112405 (2013).
[13]L. Huang, Z. Zhang, B. Chen, X. Ma, H. Zhong, and L.-M. Peng, Appl. Phys. Lett. **104**, 183106 (2014).
[14]S. Rumyantsev, G. Liu, M. S. Shur, R. A. Potyrailo, and A. A. Balandin, Nano letters **12**, 2294 (2012).
[15]S. Rumyantsev, G. Liu, R. A. Potyrailo, A. A. Balandin, and M. S. Shur, IEEE Sens. J. **13**, 2818 (2013).
[16]K. R. Amin and A. Bid, Appl. Phys. Lett. **106**, 183105 (2015).
[17]R. Samnakay, C. Jiang, S. Rumyantsev, M. Shur, and A. Balandin, Appl. Phys. Lett. **106**, 023115 (2015).
[18]M. Z. Hossain, S. Rumyantsev, M. S. Shur, and A. A. Balandin, Appl. Phys. Lett. **102**, 153512 (2013).
[19]SCCM denotes cubic centimeters per minute at standard temperature and pressure.
[20]BDScom Plasma Matrix system.
[21]A. C. Ferrari and J. Robertson, Phys. Rev. B **61**, 14095 (2000).
[22]L. Callegaro, V. D'Elia, M. Pisani, and A. Pollarolo, Metrologia **46**, 409 (2009).
[23]The current was generated by a 4.5 V NiMH battery in series with a 10 MΩ metal film resistor.
[24]The overall gain is 10^4; the cut-off frequency is about 3.3 mHz.
[25]National Instruments mod. 4462, 24 bit resolution.
[26]L. Callegaro, M. Pisani, and M. Ortolano, Metrologia **47**, 272 (2010).
[27]L. Callegaro and M. Pisani, Appl. Phys. Lett. **89**, 034105 (2006).
[28]F. Hooge, Phys. B+C **83**, 14 (1976).
[29]L. K. J. Vandamme, in *2013 International Conference on Noise and Fluctuations (ICNF)* (2013), pp. 1–6.
[30]B&W Tek i-Raman system.
[31]Typical Micro-Raman setups, with power densities above 10^4 W cm^{-2}, easily provoke the formation of additional defects in CVD graphene.
[32]G. Amato, G. Milano, U. Vignolo, and E. Vittone, Nano Res. **8**, 3972 (2015).
[33]A. C. Ferrari, J. Meyer, V. Scardaci, C. Casiraghi, M. Lazzeri, F. Mauri, S. Piscanec, D. Jiang, K. Novoselov, S. Roth *et al.*, Phys. Rev. Lett. **97**, 187401 (2006).
[34]L. Malard, M. Pimenta, G. Dresselhaus, and M. Dresselhaus, Phys. Rep. **473**, 51 (2009).
[35]A. Eckmann, A. Felten, A. Mishchenko, L. Britnell, R. Krupke, K. S. Novoselov, and C. Casiraghi, Nano Lett. **12**, 3925 (2012).
[36]C. Neumann, S. Reichardt, P. Venezuela, M. Drögeler, L. Banszerus, M. Schmitz, K. Watanabe, T. Taniguchi, F. Mauri, B. Beschoten *et al.*, Nat. Commun. **6**, 1–7 (2015).
[37]F. Tuinstra and J. L. Koenig, J. Chem. Phys. **53**, 1126 (1970).
[38]D. Teweldebrhan and A. A. Balandin, Appl. Phys. Lett. **94**, 013101 (2009).
[39]P. Mallet-Ladeira, P. Puech, C. Toulouse, M. Cazayous, N. Ratel-Ramond, P. Weisbecker, G. L. Vignoles, and M. Monthioux, Carbon **80**, 629 (2014).
[40]This phenomenon was not visible in the G peak because the electron-phonon coupling effects overwhelm the peak broadening[36].
[41]C. Casiraghi, S. Pisana, K. Novoselov, A. Geim, and A. Ferrari, Appl. Phys. Lett. **91**, 233108 (2007).
[42]N. W. Ashcroft and N. D. Mermin, *Solid State Physics* (Saunders College, Philadelphia, 1976).
[43]A. H. Castro Neto, F. Guinea, N. M. R. Peres, K. S. Novoselov, and A. K. Geim, Rev. Mod. Phys. **81**, 109 (2009).
[44]J. Lu, J. Pan, S.-S. Yeh, H. Zhang, Y. Zheng, Q. Chen, Z. Wang, B. Zhang, J.-J. Lin, and P. Sheng, Phys. Rev. B **90**, 085434 (2014).
[45]A. N. Pal, A. A. Bol, and A. Ghosh, Appl. Phys. Lett. **97**, 133504 (2010).
[46]A. Dmitriev, M. Levinshtein, and S. Rumyantsev, J. Appl. Phys. **106**, 024514 (2009).
[47]Yu. M. Gal'perin, V. G. Karpov, and V. I. Kozub, Sov. Phys. JETP **68**, 648 (1989).
[48]For example, centers that change their scattering cross section as a consequence of capture or release of an electron or a hole by the trap, see Ref. 46 and therein.